Interplay between Intra- and Intermolecular Excited-State Single- and Double-Proton-Transfer Processes in the Biaxially Symmetric Molecule 3,7-Dihydroxy-4H,6H-pyrano[3,2-*g*]-chromene-4,6-dione†

Elena Falkovskaia,‡ Vasyl G. Pivovarenko,§ and Juan Carlos del Valle*,||

Institute of Molecular Biophysics and Department of Chemistry, Florida State University, Tallahassee, Florida 32306-4380, Chemistry Department, Kyiv National Taras Shevchenko University, Volodymyrska 64, Kyiv 01033, Ukraine, and Departamento de Química Física Aplicada, C-2−203, Universidad Autónoma de Madrid, Cantoblanco, E−28049 Madrid, Spain

Received: August 1, 2002; In Final Form: December 3, 2002

The molecule 2,8-diphenyl-3,7-dihydroxy-4H,6H-pyrano[3,2-g]-chromene-4,6-dione (D3HF, diflavonol) has been synthesized. This molecule contains two mutually symmetric and identical intramolecular hydrogen-bond systems. D3HF exhibits diverse excited-state proton-transfer processes, which transform it in a novel molecule in proton-transfer spectroscopy. Ultraviolet−visible absorption and fluorescence spectroscopy have been applied to D3HF in hydrocarbon, dioxane, and protic solvents from 295 to 77 K, together with fluorescence quenching experiments. The interplay between intramolecular single-proton-transfer and intermolecular double-proton-transfer processes has been demonstrated in protic solvents. Density functional calculations (DFT) in the ground state (DFT-B3LYP) and in the singlet excited states (time-dependent DFT) have been executed for D3HF and for 3-hydroxiflavone (3HF). The theoretical calculations confirm the experimental photophysical evidence. The role of the phenyl torsion on the proton-transfer spectroscopy of D3HF and 3HF is also discussed. Contrary to previous semiempirical calculations, for the isolated 3HF molecule the most stable conformation is the coplanar phenyl ring conformation.

Introduction

The proton-transfer (PT) process has become an important issue in a great variety of fields in science and technology.[1−4] The molecule 2,8-diphenyl-3,7-dihydroxy-4H,6H-pyrano[3,2-g]-chromene-4,6-dione (D3HF, Scheme 1) has been synthesized to create two identical intramolecular hydrogen-bond (IMHB) systems in the isolated molecule under one electronic structure, thus enhancing our insight in excited- and ground-electronic-state PT processes. The structural features of D3HF offer key examples of single-PT (SPT) and double-PT (DPT) processes and their relationship on a singular molecular skeleton.

D3HF is a structural analogue of the 3-hydroxyflavone (3HF) molecule, its structure being like two phenyl γ-pyrone molecules fused with a benzene ring, thus the isolated molecule possesses a biaxial symmetry corresponding to the C_{2v} symmetry group. The D3HF molecule exhibits several photophysical similarities with 3HF. For instance, both molecules D3HF[5] and 3HF[6,7] exhibit strong PT fluorescence with vibronic structure in hydrocarbon solvents. Both their vibronic structure and the peak fluorescence wavelength are correctly predicted by time-dependent (TD) density functional theory (DFT) calculations,

SCHEME 1

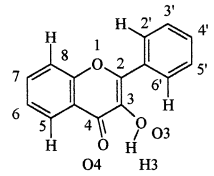

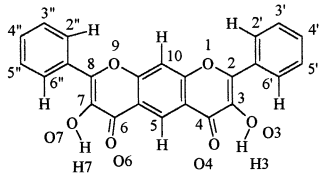

which show stationary-state energy minima in its ground electronic state (S'_o) and the first excited electronic state (S'_1). In protic solvents the PT fluorescence of 3HF has been observed as well, but accompanied by the normal tautomer (NT) fluorescence.[6,7] The behavior of 3HF in protic solvents parallels that found for the D3HF molecule, but this latter increases in complexity owing to the presence of two IMHB systems (vide infra).

The PT fluorescence of D3HF has been reported previously[5] in Decalin at 298 K and in ethanol at 77 K, and it shows peaks at 587 and 600 nm, respectively. On the basis of the TD-DFT (B3LYP) calculations for the S_1 state, and DFT(B3LYP) calculations for the S_o state, that PT fluorescence band was assigned to the intramolecular SPT fluorescence. Intramolecular DPT fluorescence of D3HF was not observed either at 298 K or at 77 K in Decalin, ethanol, and in solvent mixtures.

† Part of the special issue "George S. Hammond and Michael Kasha Festschrift". The authors wish to especially dedicate this paper to the dearest Prof. Kasha for his continuous support, his attitude to life and science which inspire us, and his versatility of talents that we admire.

* To whom correspondence should be addressed. E-mail: juan.valle@uam.es.

‡ Institute of Molecular Biophysics and Department of Chemistry. Current address: Department of Biochemistry and Molecular Biology (Lederle Graduate Research Tower, Room 913G710), North Pleasant St., University of Massachusetts Amherst. Amherst, MA 01003-9306.

§ Chemistry Department.

|| Departamento de Química Física Aplicada.

10.1021/jp021791p CCC: $25.00
Published on Web 03/07/2003

This paper aims at exploring, for the first time, the several possibilities of PT processes and their interplay that D3HF exhibits in the isolated molecule, thus resembling the gas phase, and in different solvents, as for example, Decalin, methylcyclohexane, dioxane, and alcohol.

At 298 K a long-wavelength fluorescence band is observed at ca. 566 nm in ethanol solution, and upon quick freezing at 77 K this fluorescence band shifts to 600 nm and loses its complexity. This 600 nm emission band resembles the PT fluorescence band monitored in dioxane, Decalin, and methylcyclohexane at 298 K. A most feasible interpretation is demonstrated based upon the interplay between inter- and intramolecular PT processes, together with a dynamical quenching mechanism.

The research of flavonoid compounds has led a skyrocketing increase, owing to the discovery of their biological role in plants, the disease resistance as antifungal agents or as phytoalexins, and recently their relevant contribution in human physiology and medicine.[1,8,9] Indeed, some recent experiments suggest that some flavonoids may have a value as anticancer agents.[1,10−14] These important applications of the flavonoids emphasize the necessity to understand the foundations of their activity.

Theoretical and Experimental Methods

Spectroscopy. Absorption spectra were measured at 298 K on a Shimadzu UV-2100 spectrophotometer, utilizing a thermostatized bath Medingen U6. The D3HF molecule exhibits a limited solubility and tends to aggregate in hydrocarbon solvents. To eliminate aggregation effects, sufficiently dilute solutions have been employed. Absorption spectra from 298 to 106 K were recorded with the aid of a Varian Cary 5 spectrophotometer and a thermostatized cooling system Oxford Optistat DN. The emission spectra at 298 K were recorded with a Fluorolog-2, an SLM Aminco 48000, and an SLM Aminco Bowman (Series 2) spectrofluorometers, and were corrected for instrumental sensitivity, except for those emission spectra in Figure 8. Some luminescence measurements at 77 K were obtained by quick-freezing in a low-temperature accessory. The luminescence spectrum series from 298 to 77 K were recorded by slow freezing, using the cooling system Oxford Optistat DN coupled to the SLM Aminco Bowman (Series 2) spectrofluorometer. At 77 K, the D3HF ethanol matrix was not adequately transparent because of cracking, and the corresponding absorption spectrum could not be recorded owing to an excessive light scattering.

The solvents used were of spectrophotometric quality, and were checked for the impurities. For the sake of checking and avoiding the photodegradation of the sample, the irradiation times have been shortened and absorption spectra have been recorded before and after the experiments. No photodegradation of the samples was observed in the experiments reported in this paper.

Synthesis. The molecule 2,8-diphenyl-3,7-dihydroxy-4H,6H-pyrano[3,2-g]-chromene-4,6-dione was synthesized by the Algar−Flynn−Oyamada reaction.[15] For this purpose 2,4-dicinnamoylresorcinol was threaded by hydrogen peroxyde in alkaline water-ethanol solution. The precipitate obtained after acidification was purified upon several recrystallizations from chloroform. The yellow crystals obtained possess mp 323−324 °C (323 °C according to ref 15). The purity of D3HF was checked by TLC and ^{1}H NMR methods. Mass, IR, and ^{1}H NMR spectroscopies confirmed authenticity of D3HF. The characteristic spectroscopic data values of the ^{1}H NMR spectrum, measured at 200 MHz frequency in DMSO-d_6 with TMS as internal standard, are displayed below. These data values are presented in δ-scale, and abbreviated as signal position in ppm, and shape of a signal (s = singlet; d = doublet, m = multiplet, and b = broad). The coupling constant, number of protons, and their position in the molecule (in brackets) are also reported: 9.77bs, 2H (OH-3, OH-7); 8.76s, 1H (H-5); 8.22d, 8 Hz, 4H (H-2′,6′,2″,6″); 8.02s, 1H (H-10); 7.56m, 6H (H-2′,3′,6′,2″,3″,6″).

Theoretical Calculations. All the calculations were executed with the split valence 6-31G(d,p) basis set, commonly named as 6-31G**, which introduces d polarization functions on heavy atoms and p polarization functions on the hydrogen atoms.[16]

The ground-electronic-state (S_o) calculations with geometry optimization were executed using density functional theory (DFT) with the B3LYP hybrid functional. Stationary points on the S_o potential energy (PE) curve were further characterized with calculations of vibrational frequencies. The S_o stationary minima obtained represent fully optimized geometries without frozen coordinates with all the vibrational frequencies as positive. The PT PE curves were obtained by stretching only one of the O−H distances (stepwise mechanism) or both O−H distances (concerted mechanism), and thus fixing those distances and allowing the remaining intrinsic coordinates to be optimized.

The excited-state calculations were executed using two different methods. In method A, theoretical calculations at the B3LYP-DFT level for S_o, and at the CIS level (without geometry optimization) over the B3LYP-DFT fully optimized geometry for calculating the excited-state electronic densities, and dipole moments. In method B, time-dependent (TD) DFT (B3LYP) methodology was executed to obtain the electronic transition energies to be added to the corresponding DFT (B3LYP) energies. Therefore, the PT PE curves have been built with the methodology B. All the calculations have been performed with the aid of the Gaussian 98, and the Spartan 4.1 programs.[17]

Results and Discussion

PT processes are connected to molecular structure,[4,18,19] thus revealing a fundamental theme in chemistry and physics. Within an IMHB system an H-donor and an H-acceptor are linked so that an intramolecular PT reaction might be produced in the ground state (GSIPT) or in the excited state (ESIPT): the electrostatic and covalent character of the IMHB link has been demonstrated.[20] However, there is not a clear-cut relation between hydrogen bond strength and the occurrence of a PT process.[18,19] For example,[19] some molecules which possess strong IMHB (i.e., methyl 1-hydroxy-2-naphthoate and methyl 2-hydroxy-1-naphthoate) do not undergo ESIPT nor GSIPT mechanisms, and however, their analogue (i.e., methyl 2-hydroxy-3-naphthoate) with a weaker IMHB does undergo ESIPT mechanism. The key point to better understand this subject lies in the acidity and basicity change undergone by the H-donor and H-acceptor groups upon excitation, respectively. There exists a requirement by which upon photoexcitation both donor and acceptor groups of each hydrogen bond undergo a large increase in acidity and basicity, respectively.[21] If only one component of the donor−acceptor pair undergoes a large increase, but not the other, the PT process will be hindered. As can be seen in the HOMO−LUMO orbitals of the D3HF molecule (Figure 1) the increase of acidity of the hydroxy group is accompanied by an increase in basicity of the carbonyl group within the IMHB. Thus, the three HOMO−LUMO pairs in the S_1 state (Figure 1a−c) depict two intramolecular PT processes, SPT and DPT, which may occur, and compete with each other.

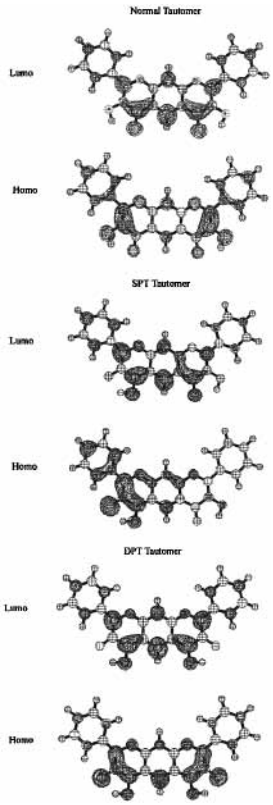

Figure 1. Homo-Lumo (π,π^*) orbitals which depict the S_1-state configuration for the normal tautomer (NT), the single-proton-transfer (SPT) tautomer, and the double-proton transfer (DPT) tautomer of D3HF.

The novel design and characterization of the D3HF molecule, which undergoes several PT processes (vide infra), will definitely provide valuable information on the PT spectroscopy of the 3HF molecule and its analogues, and on the SPT and DPT processes in general.

Absorption and Molecular Structure of D3HF in Isolated Molecule and in Hydrocarbon Solution. The absorption spectrum of D3HF is batochromically shifted ca. 40 nm in comparison to the absorption spectrum of 3HF, Figure 2. In accordance with the TD-DFT calculations, the Franck−Condon electronic transition $S_o(NT)\rightarrow S_1(NT)$ is π,π^* in nature with a predominant HOMO−LUMO configuration, as well as the other two electronic transitions $S_o'(SPT)\rightarrow S_1'(SPT)$ and $S_o''(DPT)\rightarrow S_1''$-(DPT).

The calculations obtained at the TD-DFT level show that the transition dipoles are oriented perpendicular to each other, and lie along the *y*-axis for S_1 (L_a), and along the *x*-axis for S_2 (L_b). This transition dipole orientation distribution matches the transition dipole orientation of anthracene and tetracene.[22] Therefore, the calculated perpendicular mutually polarization of transition moments obeys the symmetry requirement of the D3HF molecule, which resembles that of anthracene and tetracene.

The first question addressed when calculating the D3HF molecule is, what geometry does it possess? The main point is whether the phenyl rings are in or out of the aromatic plane of the heterocyclic moiety. The phenyl torsion feasibility in the D3HF molecule has been studied (Theoretical Methods Section) in the S_o (B3LYP-DFT) and in the S_1 states (TD//B3LYP-DFT). The theoretical results indicate that the D3HF molecule is planar in all the electronic states, thus presenting coplanar phenyl rings as the most stable geometry, with all the vibrational frequencies

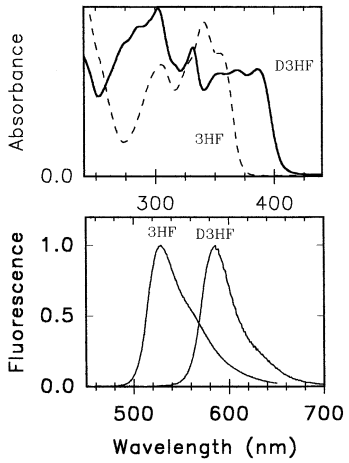

Figure 2. Upper: Absorption spectra of the 3HF and D3HF molecules in Decalin. Lower: Fluorescence spectra of 3HF ($\lambda_{exc} = 340$ nm) and D3HF ($\lambda_{exc} = 370$ nm) in Decalin.

as positive for the stationary minimum-energy states of the NT, SPT, and DPT tautomers in S_o. However, the energy difference between out-of-plane and in-plane phenyl ring configurations is very small. Indeed, for the S_o state of NT the fully optimized geometry with one of the phenyl rings anchored at 5° out of the plane possesses an energy value of only 0.02 kcal/mol higher than that of the in-plane phenyl conformation. Thus, within the Boltzmann distribution at room temperature, there might be a set of out-of-plane phenyl conformations in equilibrium with the coplanar one. Upon excitation, the potential energy curve for the phenyl torsion becomes steeper (0.04 kcal/mol for a 5° dihedral phenyl torsion vs the coplanar conformation) than in the S_o state, thus indicating that the coplanar conformation is more favored in the S_1 state, though the energy difference is still very small.

Also, upon excitation, as can be seen in the HOMO−LUMO orbitals (Figure 1), there exists a greater contribution in the inter-ring phenyl−chromone bond, gaining a larger double-bond character and thereby posing a hindrance to phenyl torsion. The same results obtained above for D3HF are applied to 3HF; the most energetically favored conformation yields the in-plane phenyl ring one, though the out-of-plane conformational energy is only slightly higher. The phenyl ring coplanarity in 3HF at the DFT level agrees with the optimized geometry found at the HF level,[23] and contradicts previous theoretical results obtained by using the semiempirical AM1 method,[24] which reported a saddle point in S_o for the in-plane (coplanar) phenyl ring 3HF conformation. For 3HF, X-ray data have reported a phenyl-chromone dihedral angle of 5.5°.[24] The intermolecular forces in the crystal packing may force the 3HF-phenyl ring to be out of planarity. These interactions are to be absent in gas phase or hydrocarbon solution. Conversely, in alcohol solution the phenyl ring may be forced to be out of planarity owing to the complexity of hydrogen bonding solute−solvent interactions (vide infra).

Does the phenyl torsion significantly change the energetic of the ESIPT? The calculated in-plane and out-of-plane conformation energies for D3HF lead to a small energy difference as stated above. Also, the ESIPT process for D3HF ought to be very fast. The ESIPT time for 3HF in S_1 has been measured to be 240 fs.[25] The same order of magnitude for the PT rate of D3HF may be assumed owing to structural similarities, and that in dried Decalin and methylcyclohexane solution the only emission observed corresponds to the PT fluorescence (vide infra). The high PT rate in S_1 supports that the phenyl torsion

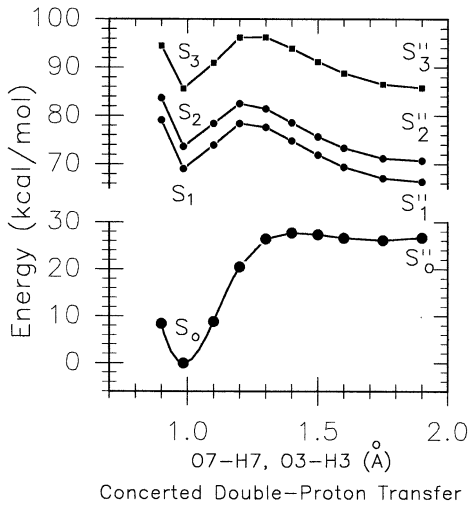

Figure 3. Proton-transfer potential-energy curves of D3HF for the concerted mechanism.

motion, which is an order of magnitude slower than the measured ESIPT rate for 3HF,[26] does not influence significantly the ESIPT process.[23] In accordance with this conclusion, the PT PE curves for D3HF have been calculated from a coplanar phenyl conformation either for the S_o state or for the excited-singlet-electronic states.

The existence of the SPT tautomer of D3HF in the ground state seems to be unlikely in view of the 13 kcal/mol energy difference with the NT species. The same conclusion has been drawn for the 3HF molecule; its PT tautomer absorption has not been monitored in the ground state even under drastic conditions at low temperature.[27−30]

The presence of two five-membered intramolecular hydrogen bonds of the carbonyl-hydroxy type in D3HF poses new avenues to PT spectroscopy, thus offering a more complex photophysical picture than that of the 3HF molecule.

Emission of the D3HF Molecule in Hydrocarbon Solution. The D3HF emission in Decalin is depicted in Figure 2 in comparison to that of the 3HF molecule. D3HF preserves some of the peculiar properties of the 3HF. (I) Both molecules exhibit intramolecular PT emission.[5,31] The energy difference between the absorption and the PT emission spectra yields ca. 9200 cm^{-1} for 3HF, and 8800 cm^{-1} for D3HF (Figure 2). (II) The intramolecular PT tautomer of 3HF was assumed to involve a double-minimum-potential barrier, with subsequent experimental demonstration given by the sharpened vibronic structure posed by the 3HF PT emission in Shpol'skii matrixes at 77 K,[32] and by argon matrixes at 10 K.[25] The D3HF molecule also poses vibronic structure in the fluorescence spectrum, which matches the theoretical results that show stationary-state energy minima either in the S'_1, or in the S'_o states of the PT PE curves. The excitation spectra (not shown) of the fluorescence emission resemble the respective absorption spectra.

Proton-Transfer Processes of D3HF in the Isolated Molecule and Hydrocarbon Solution. Owing to the presence of two IMHBs in the D3HF skeleton, single- or double-PT processes may be occurring. Figure 3 shows the concerted DPT process for the S_o and the first three excited singlet states. The ground state exhibits two minima for both the NT and the DPT species with positive vibrational frequencies. The S_o PT process is endothermic with a barrier of ca. 26 kcal/mol for the direct DPT process, and of 1.6 kcal/mol for the reverse DPT process. The S_1 and S_2 states show exothermic DPT processes, thus allowing this concerted mechanism to occur. To the converse,

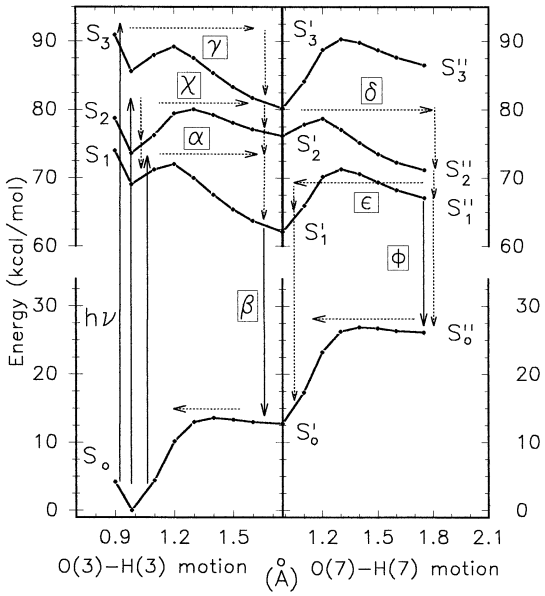

Figure 4. Stepwise proton-transfer processes of the D3HF molecule calculated with DFT for the S_o state, and with TD-DFT for the singlet excited states.

the S_3 state exhibits an endothermic DPT process for the same O−H distances. However, comparison of the PT barriers of the concerted (Figure 3) and the stepwise mechanisms (Figure 4) shows lower PT barriers (concerted, S_1-S_1'', 9.3; S_2-S_2'', 8.9; and S_3-S_3'', 10.6 kcal/mol; vs stepwise, S_1-S_1', 2.9; S_2-S_2', 6.4; and S_3-S_3', 3.6 kcal/mol) for the latter mechanism.

Figure 4 indicates that the SPT minimum in S_1' is more stable than that of the DPT minimum in S_1'', thus trapping the excited-state population, and impeding the second PT process to occur. The fluorescence peak at 587.5 nm in Decalin, and at 582 nm in methycyclohexane at 298 K, corresponds to the theoretically calculated $S_o'-S_1'$ SPT electronic transition of 579 nm (Figure 4) and thus was assigned to the SPT excited-state electronic transition. The intramolecular DPT emission, which should have appeared at about 698 nm (TD-DFT), has not been observed at 298 K nor at any other temperature up to 77 K, in mixtures of methylcyclohexane and 2-methyltetrahydrofuran (2:1), methylcyclohexane/2-methyltetrahydrofuran/ethyl iodide (2:1:1), and ethanol, as reported previously.[5] Other solvent mixtures have been checked in order to unravel the existence of the D3HF DPT emission (Table 1), however, all attempts failed to reveal that emission, though the DPT emission may lie underneath the long-wavelength tail of the SPT emission, thus possessing a very low fluorescence quantum yield.

In sum, the S_1 state will lead to a SPT process, the S_2 state provides grounds for a DPT stepwise mechanism via a stable SPT intermediate in S_2', and the S_3 state exhibits a SPT process similar to that of the first excited singlet PE curve (Figure 4).

Figure 4 gathers some routes that could be guiding the PT processes of the D3HF stepwise-type diagram in the singlet manifold. The SPT fluorescence process is represented by the $\alpha-\beta$ route, in which upon excitation a SPT process (α) occurs, with a subsequent intramolecular vibrational relaxation, and then decaying by emission (β) to the S_o' state. Nonradiative process in the β route, by internal conversion or intersystem crossing may be competing with the emission decay. A fraction of SPT species in S_1' may be produced by reverse PT (ϵ) from DPT species in S_1''. This DPT species may be generated through the $\chi-\delta$ route in S_2, via a stable SPT intermediate (S'_2) along a stepwise mechanism, and following the back PT (ϵ) route. This process seems to possess a low probability since the theoretical

TABLE 1: Absorption and Emission Wavelength Maxima of D3HF in Several Solvents at 298 K (*RT*) and 77 K, and Half-Width (HW) of the PT Emission at *RT*

solvent	λ (nm), ABS	λ (nm), EM *RT*: NT/PT	λ (nm), EM 77K: NT/PT	HW (cm^{-1}) *RT*
decalin	386	-/587.5		1139
methylcyclohexane (MCH)	385	-/582		1165
1,4-dioxane	386	453/600		1503
ethyl ether/MCH (2:1)	372, 384	440/599	416,441/604	1353
ethyl ether/*n*-pentane (2:1)	369	439/598	415,442/605	1368
EPA	357, 375	475/606	422,444/602	
ethanol	360	484/566	442/602	2556
methanol/ethanol (9:1)	345, 359	488/564	450/602	
propylene glycol	358−374, 352	488/562	445/606	

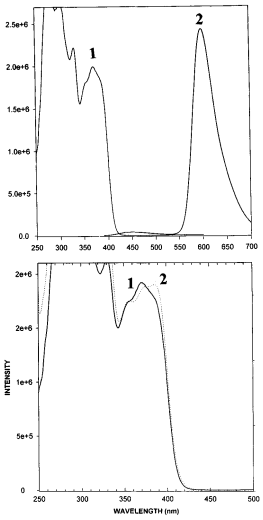

Figure 5. Upper: Excitation (1, monitoring at 620 nm) and fluorescence (2, exciting at 386 nm) spectra of D3HF in dioxane at 298 K. Lower: Excitation (1) and absorption (2) spectra of D3HF in dioxane at 298 K.

SCHEME 2

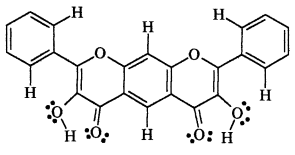

Close-form with in-plane phenyl rings

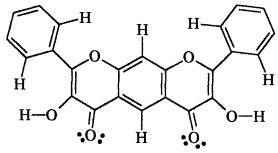

Open-in: open-form with in-plane phenyl rings and hydroxy groups

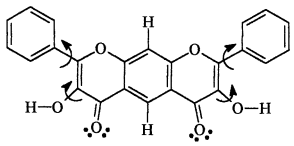

Open-out: open form with out-of-plane phenyl rings and hydroxy groups

calculations show that the electronic density on the oxygen atoms, O3 and O7, decreases abruptly upon excitation, thereby not favoring the reverse DPT to happen. Also, Figure 1 shows the HOMO−LUMO orbitals for the DPT tautomer, in which the LUMO orbital contribution on the oxygens O3 and O7 is zero. As mentioned above, the DPT fluorescence process (ϕ) through either the first or second singlet excited states has not been observed experimentally. In addition, the PT $\chi-\delta-\epsilon$ route will not be favored when competing with the internal conversion between the $S_2-S_2'-S_2''$ and the $S_1-S_1'-S_1''$ states. Also, the SPT γ route seems to be unlikely owing to a most probable fast internal conversion from S_3 to S_2 and to S_1.

The D3HF Molecule in Dioxane Solution. The D3HF fluorescence spectrum at 298 K in dioxane consists of two bands, Figure 5. The first fluorescence band at ca. 453 nm corresponds to the NT fluorescence. It does not exhibit vibronic structure and its excitation spectrum resembles the absorption spectrum. The second fluorescence band at 600 nm is assigned to the SPT fluorescence; its excitation spectrum also resembles the absorption spectrum in dioxane solution, Figure 5. This evidence exemplifies one of the rare cases in which both the NT and the PT fluorescences come from the same absorbing species in the ground state. Therefore, both fluorescences may be ascribed to the close-form NT species of the D3HF molecule (Scheme 2).

The disruption of the five-membered IMHB is more feasible than a six-membered one by H-accepting solvents. Therefore, it was reasonable to expect that in such a solvent as dioxane, the solute−solvent interactions might force the opening of the five-membered IMHB, thereby generating the open-form species. The existence of the open-forms species was observed neither in the excitation and emission spectra nor in the absorption spectra of D3HF in dioxane. The absorption spectrum of D3HF in dioxane resembles that recorded in hydrocarbon solution.

It is suggested that the larger solvent polarity of dioxane compared to hydrocarbon stabilizes the S_1 stationary minimum-energy state of NT, thereby favoring the fluorescence decay of the close-form NT species. The calculated dipole moments of the close-form NT molecule yield 5.02 D for the S_o state, and 6.98 D for the S_1 state. This means that the increase of solvent polarity tends to shift D3HF absorption and emission bands to the red. The orientation of both dipole moments of the S_o and S_1 states does not change and lies along the C5 and C10 carbons in the *y*-axis. Thus, the solvent relaxation effect for the close-form NT emission is expected to be negligible.

The DFT(B3LYP) calculations with 6-31G** basis set and full geometry optimization have resulted in that the open form of D3HF with in-plane phenyl rings (open-in, Scheme 2) is 30.2 kcal/mol less energetically favored than the close-form species (Scheme 2). Nevertheless, the open-in optimized geometry exhibits three negative vibrational frequencies, and thus it does not represent an energy minimum.

On the other hand, when the phenyl ring is out of planarity (open-out, Scheme 2) a final phenyl-chromone dihedral angle of 35.3° (i.e., C6″−C1″−C8−O9, with full geometry optimization) is obtained. This new open form (open-out) is 20.1 kcal/mol less stable than the close-form (Scheme 2). The open-out species also possesses the hydroxy groups out of the chromone plane (i.e., H7−O7−C7−C8, −14.8°), and provides 10.2 kcal/mol energy stability in comparison with the open-in form

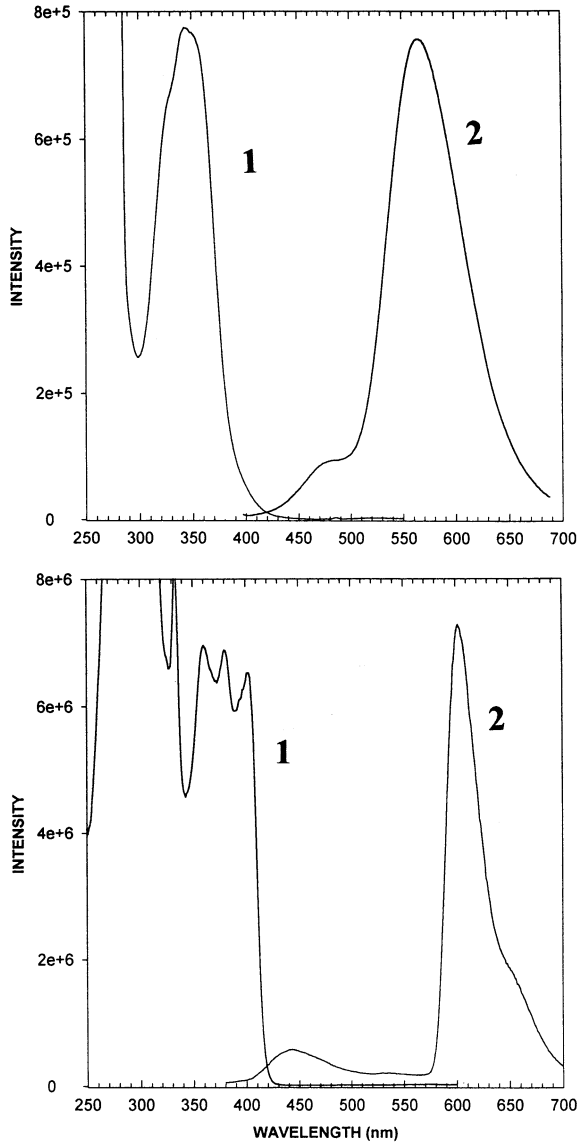

Figure 6. Upper: Excitation (1, monitoring at 566 nm) and fluorescence (2, exciting at 349 nm) spectra of D3HF in ethanol at 298 K. Lower: Excitation (1, upon monitoring at 610 nm) and Fluorescence (2, upon excitation at 360 nm) spectra of D3HF in ethanol at 77 K.

species. The vibrational frequency analysis reveals all positive vibrational frequencies for the open-out structure.

The 20.1 kcal/mol energy difference instability of the open-out species compared to the close-form NT species may explain why the open-form species is not observed in dioxane solution. The stability of the open-form species is associated with the solvation energy of this species. It is expected that in other solvents the open-form species may be generated, for example, via stronger intermolecular hydrogen bonds, which may provide greater solvation effect, and greater energy stability.

It has been demonstrated[33] that the solvatochromism of the PT fluorescence of 3HF depends basically on three factors, polarity, and polarizability, and basicity of the solvent used, acidity having a negligible contribution. If a more basic solvent than dioxane (i.e., ethanol) is employed, the IMHBs of D3HF may be disrupted and the open-form species would be generated.

The D3HF Molecule in Ethanol Solution. At 298 K, a very intriguing emission spectrum is recorded, which seemingly shows only two emission bands centered at ca. 480 and 566 nm (Figure 6). The 566 nm band displays an anomalous half width of 2556 cm^{-1}, which is twice larger than that of the SPT

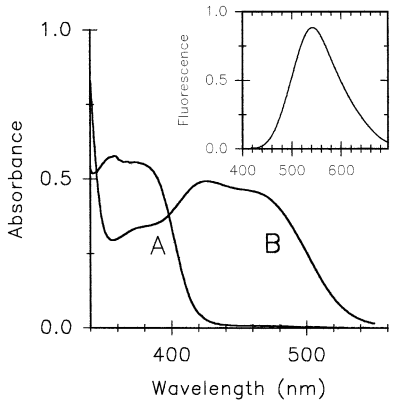

Figure 7. Absorption spectra of D3HF in ethanol (A), and in ethanol with sodium ethoxide (B). Inset: anion fluorescence spectrum (λ_{exc} = 390 nm) of D3HF in the ethanol/sodium ethoxide solution at 298 K.

fluorescence of D3HF (Table 1) in methylcyclohexane (1165 cm^{-1}), or in dioxane (1503 cm^{-1}). The excitation spectrum of the 566 nm band upon monitoring at 540 nm is blue-shifted in comparison with the absorption spectrum. While the excitation spectra by monitoring at 610 nm appears to be similar to the absorption spectrum. The Stokes' shift between the excitation spectra and the 566 nm emission band yield about 8500 cm^{-1}. Owing to the blue shifted excitation spectrum of the 566 nm emission and to the large Stokes' shift, we suggest that this emission is originated by the open-form absorbing species, which may undergo an intermolecular PT process upon excitation. The TD-DFT calculations yield a S_o-S_1 transition for the open-out species of 374 nm, which is blue shifted compared with the S_o-S_1 transition of 414 nm for the close-form species.

The absorption spectrum shows another band centered at 470 nm, which possesses a small absorbance. Upon exciting at 470 nm, a new single emission band develops, thus peaking at 540 nm. For the purpose of determining the nature of this long-wavelength absorption band, a fresh solution of D3HF ethanol was formed and a small amount of sodium ethoxide was added. By this procedure, the double anion of D3HF was totally generated in the ground state (Figure 7). The absorption spectrum changes dramatically, and shows a long-wavelength absorption band centered at 470 nm. Upon excitation the absorbing species yields a fluorescence band that resembles the D3HF emission band at 540 nm in ethanol. The fluorescence of the D3HF ethoxide/ethanol solution exhibits an excitation spectrum that matches the corresponding absorption spectrum. The long-wavelength absorption band in ethanol may be thus ascribed to the solvated anion species. Thus, the long-wavelength fluorescence of the D3HF in ethanol may experience a contribution from the ground-state anion of D3HF, and thus artificially increase the half-width of the long-wavelength fluorescence band.

At first glance, the fluorescence spectrum of D3HF in ethanol at 77 K presents a puzzle. When lowering quickly the temperature up to 77 K, a spectrum is obtained which poses two fluorescence bands centered at about 442, and 602 nm, and a negligible peak at 540 nm (Figure 6). The 540 nm peak of emission is almost hidden in the tail of the other two emissions. The 602 nm fluorescence resembles the intramolecular SPT fluorescence monitored in methylcyclohexane, Decalin, dioxane, and ethyl ether/hydrocarbon mixtures, thus possessing a half width of ca. 1200 cm^{-1}. The excitation spectra at 77 K upon monitoring the emission at 610, 515, and 442 nm exhibit some differences.

SCHEME 3

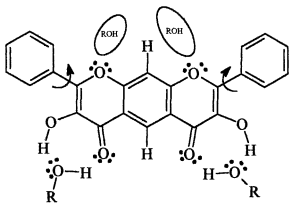

Solvent-solute (2:1) close-form with out-of-plane phenyl rings

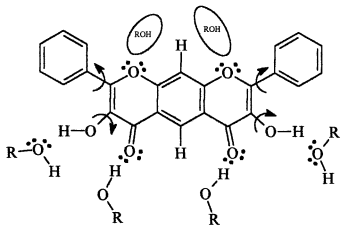

Open-form with out-of-plane phenyl rings and O-H groups

Additionally, we observed an excitation wavelength dependence of the emission spectra at 77 K. Thus, upon excitation at 360, 380, and 427 nm the intensity of the SPT fluorescence at 602 nm diminishes progressively. This SPT emission is, upon excitation at 427 nm, lower in intensity than the 442 nm emission band. In addition this 442 nm band develops vibronic structure (two peaks at about 442 and 470 nm), and the 540 nm shoulder is seemingly suppressed. This wavelength dependence may be interpreted in terms of a composite absorption band, with several species generated, that is, open-out species (Scheme 3), close-form species, and anion species. The close-form species may be those depicted in the Schemes 2 and 3; thus, it comprises a five-membered IMHB close-form and an intermolecular complex (2:1) solvent−solute close-form, respectively.

Furthermore, it is noteworthy to mention that the fluorescence intensity decreases abruptly in ethanol as compared to dioxane, and hydrocarbon solution at room temperature.

Absorption and emission experiments of D3HF in other alcohol solutions as EPA (ethyl ether/isopentane/ethanol, 5:5:2), methanol/ethanol (9:1), and propylene glycol have manifested the same behavior as that observed in ethanol either at 298 K or at 77 K.

For the sake of unraveling the nature of the 566 nm fluorescence band in alcohol solutions, a dioxane/ethanol titration at 298 K and low-temperature absorption and emission spectra have been measured (298−77 K).

Switching between Intra- and Intermolecular PT Processes in Alcohol Solution. The titration of D3HF in dioxane with ethanol is represented in Figure 8. It shows the dramatic decrease of the SPT emission with increasing the concentration of ethanol from 8.30×10^{-7} M to 14.14 M. The emission band of NT is also quenched, though to a smaller extent. The decrease of the SPT emission is accompanied by the appearance of a new emission band centered at 540 nm at high ethanol concentration. At 14.14 M concentration of ethanol, the resultant emission band peaks at 566 nm, and possesses a large half-width of about 2500 cm^{-1}. The SPT fluorescence has decreased about 90 times on going from pure dioxane to dioxane containing 14.14 M concentration of ethanol. This experiment reveals a clear-cut quenching of the SPT and NT emission with ethanol addition. Therefore, the 566 nm fluorescence found in solutions with alcohol content is composed of two bands: the intramolecular SPT fluorescence, and the fluorescence peaking

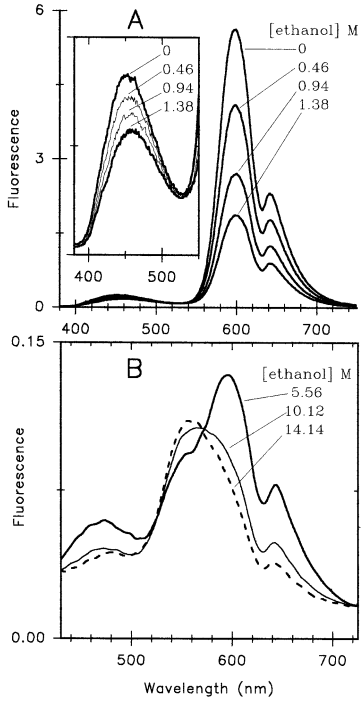

Figure 8. A: Fluorescence (λ_{exc} = 370 nm) quenching of D3HF in dioxane with addition of several ethanol quantities (0, 0.46, 0.94, and 1.38 M). Inset: enlargement of the first emission band. B: Fluorescence quenching of D3HF in dioxane with addition of large concentrations of ethanol (5.56, 10.12, and 14.14 M). These spectra are not corrected for instrumental sensitivity.

at 540 nm that may be assigned to the fluorescence of the solvated double-anion or single-anion emission (vide infra). This 540 nm emission may be mainly produced because of the excited-state intermolecular PT process. The excitation spectrum of this last band is blue shifted with respect to the absorption spectrum and thus could be due to the open-form species. Thus, it is suggested that the excited-state anion species is generated by two pathways: (I) from the ground-state solvated anion (as a minor contribution) and (II) upon excitation of the ground-state open-form species (as a great contribution) that undergo intermolecular PT generating an excited-state solvated anion-type species, which fluoresces at ca. 540 nm.

Low-Temperature Experiments from 295.4 to 77 K in Ethanol Solution. The fluorescence behavior from 295.4 K up to 160 K seems to be dominated by the increase of fluorescence intensity of the intramolecular SPT emission band vs the anion emission. This close-form SPT emission increase does not correlate with the corresponding absorption increase observed when decreasing the temperature (Figure 9), and it thus illustrates a dynamical quenching effect. Because the quencher and the fluorophore require physical contact, the excited-state collitional quenching process is diffusion-controlled, and is impeded when lowering the temperature, the SPT fluorescence intensity increases. This dynamical quenching may have distinct origins, among others: (I) exciplex formation and (II) the phenyl-torsion mechanism. Exciplex formation has been invoked to explain the quenching of the 3HF PT emission in alcohol, or in hydrocarbon with addition of small amounts of water, or alcohol.[34] On the other hand, the phenyl torsion does not seem to be coupled to the ESIPT process of the 3HF molecule, owing to the lack of viscosity dependence of the ESIPT rate.[23]

Also small amounts of a ground-state complex produced by the close-form species of D3HF and ethanol molecules may develop a static quenching. Intermolecular solvent−solute

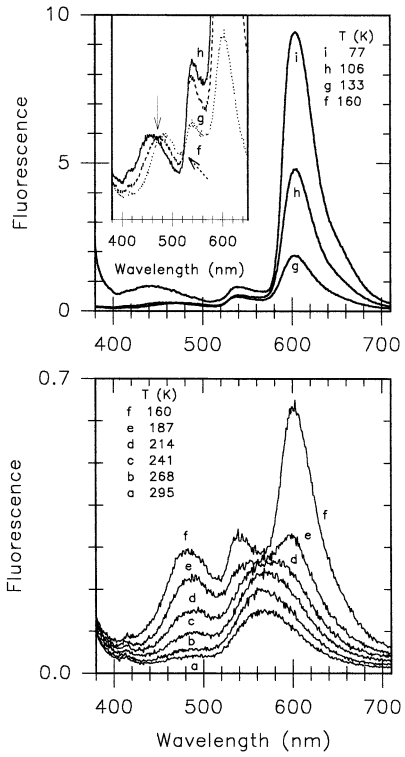

Figure 9. Fluorescence of D3HF in ethanol (λ_{exc} = 370 nm) as a function of temperature from 295 K (a) to 77 K (i). Inset: enlargement of the spectra f (160 K), g (133 K), and h (106 K).

hydrogen bonds with the close-form NT species may generate complexes. The static quenching would not have disappeared with decreasing the temperature, and thus it is expected to be in a minor contribution.

Below the freezing point of ethanol (159.05 K) the following fluorescence changes are prominent: (I) the large increased of the intramolecular SPT emission, (II) the increase of the NT emission, and (III) the blue shift of the NT emission from 484 nm at 160 K to 442 nm at 77 K, ca. 1950 cm^{-1} (Figure 9).

On one hand, the NT fluorescence spectrum is devoid of vibrational structure. The loss of vibrational structure induced by alcohol was attributed to formation of an excited-state complex (exciplex) in the 3HF[34] and indole[35] molecules. For the latter case, it was conclusively demonstrated[36] that the fluorescence changes, with an isoemissive point, observed in the 1-methylindole molecule in isooctane with addition of small concentrations of polar solvents as butanol or ethyl acetate were due to ground-state complex formation. Slight changes in the absorption spectra were linearly correlated with the fictitious exciplex emission changes. The fluorescence quenching of 1-methylindole would not present a diffusional character, and thus, no changes in the emission spectrum with lowering the temperature would have appeared.

As one may see in Figure 10, the absorption profile of D3HF changes with decreasing the temperature from 295 to 106 K. The vibronic structure is enhanced, in addition to a red shift of the shoulder at 386 nm that becomes a peak at 400 nm. In Figure 1 of the Supporting Information, the absorption spectra in Decalin and dioxane at 298 K, and ethanol at 298 and 106 K are depicted for comparison. The decrease of the temperature from 298 to 106 K for the absorption spectrum in ethanol leads to a red shift of 900 cm^{-1} compared to that absorption spectrum in Decalin, and to the gain of vibrational structure. This behavior has been also observed in the mixture ethyl ether/*n*-pentane and may be tentatively explained by an interplay between the close-

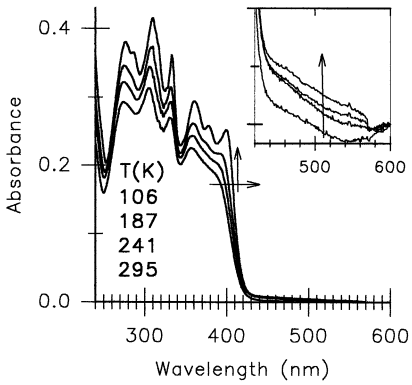

Figure 10. Absorption spectra of D3HF in ethanol as a function of temperature from 295 to 106 K. The arrows indicate the batochromic and hipsochromic changes observed. Inset: enlargement of the absorption region between 420 and 600 nm.

form complexes of NT with the solvent used (Scheme 3) and NT close-form species (Scheme 2). Nevertheless, more experiments should be necessary to shed light on this point.

Characterizing the Fluorescence Quenching of D3HF. The fluorescence of D3HF in dioxane was quenched by the presence of different amounts of ethanol, and a corresponding Stern−Volmer analysis was undertaken for the NT fluorescence emission. The ratio of fluorescence quantum yields exhibit an excellent linear relationship vs the ethanol concentration, with a correlation coefficient of $r = 0.998$, $F_o/F = 1.010 + 0.323$ [ethanol] (Figure 2 of the Supporting Infomation). Thus, the fluorescence quenching of NT is dynamical owing to excited-state interactions between the ethanol molecules and the D3HF molecule. In contrast, the PT fluorescence quenching illustrates a quadratic dependence (Figure 2 of the Supporting Infomation), which could have been ascribed to a contribution from both static and dynamical quenchings, eq 1, $F_o/F = 0.997 + 0.519$ [ethanol] + 0.671 [ethanol]^2 ($r = 1.000$). Conversely, the quadratic dependence obtained does not match the combination of static and dynamical quenchings: $F_o/F = 1 + (K_D + K_s)$-[ethanol] + $(K_D K_s)$[ethanol]^2. The dynamical and static bimolecular quenching constants, K_D and K_S, respectively, cannot be determined from eq 1, the two solutions of the quadratic equation yield imaginary values. Positive deviations from the Stern−Volmer equation are observed when the extent of quenching is large. The SPT fluorescence quenching may be 2-fold: (a) ethanol molecules quench a fraction of the NT species, and (b) another fraction undergoes a PT reaction, and a part of the SPT molecules are subsequently quenched. This may imply that the quenching process of a fraction of close-form NT is faster than the PT process. This explanation may rationalize the quadratic dependence, and thus, the principal source of quenching would be dynamical for both the NT and the SPT fluorescences.

An additional explanation relies on the quenching by ethanol aggregates. These aggregates are to be more effective quenchers than monomers because they may form stronger hydrogen bonds, thus also presenting a diffusional character.

As the temperature is lowered from 295 to 77 K in a D3HF ethanol solution, the fluorescence intensity of the SPT emission band increases about 90 times. These experiments emphasize the diffusional nature of the quenching, which is proper of the dynamical quenching. Furthermore, from Figure 9 one may extract information on the bimolecular quenching constants ($K_D = K_q\tau_o$) at each temperature, which may be proportional to the ratio f_o/f ($f_o/f = 1 + K_q\tau_o$ [ethanol]), where f_o represents the fluorescence quantum yield without quenching action (at 77 K,

as an approximation), and *f*, the quantum yield with quenching action (at any other higher temperature). The quencher concentration [ethanol] is kept constant. If the quenching is dynamical, or diffusion controlled, the plot of f_o/f should be linear with the ratio T/η,[37] T being temperature (in *K*), and η equal to viscosity (in cp). References 38 and 39 gather the viscosity parameters in ethanol for 25 temperatures, from 175.04 to 346.72 K. These data obey the Andrade equation with $r = 0.999$, that is, $\log(\eta) = 680.01/T - 2.25$. By interpolating the temperatures used, above of the freezing point of ethanol (295, 268, 241, 214, and 187 K), the viscosity values are obtained with great accuracy. As a result, an excellent linear relation is found with $r = 0.998$ for the SPT fluorescence quenching, $f_o/f = 23.22 + 0.23\ T/\eta$ (Figure 2 of the Supporting Infomation). In conclusion, both fluorescence bands NT and SPT show a definitive dynamical quenching. Further, as the alcohol content of the dioxane solution is sufficiently large, the open-form species and the anion species are generated in the ground electronic state.

A Mechanism for Excited-State Dynamical Quenching of the Close-Form PT Emission of D3HF in Alcohol Solution. It is proposed that at room temperature, the dominant conformation of D3HF is ascribed to the close-form species with the out-of-plane phenyl rings (Schemes 2 and 3). The solvated open-out species (Scheme 3) absorb to the blue of the close-form conformation; however, the absorption spectrum in ethanol is not blue-shifted with respect to that in methylcyclohexane or Decalin. Thus, there might be a fraction of open-form species but in a minor contribution. Emission from the open form species has not been observed.

The open-form species may be polysolvated (Scheme 3) in the ground state at sufficiently large concentrations of alcohol, and upon excitation undergoes the intermolecular PT process. Thus, the fluorescence at about 540 nm comes from the solvated double-anion or single-anion type species, generated because of an increase of the acidity of the O−H groups in the excited electronic state of D3HF, and the subsequent intermolecular PT process. The excited-state single-anion formation has been discarded because the TD-DFT theoretical calculations predict its S_o-S_1 electronic transition at 1250 nm. However, the double-anion emission is theoretically predicted at 587 nm (observed at about 540 nm in ethanol), thereby overlapping the SPT emission located theoretically at 579 nm (experimentally, at 587.5 in Decalin, and at 600 nm in dioxane). The DFT geometries of the single-anion and double-anion species have been optimized, and exhibit all the vibrational frequencies as positive.

The fluorescence shift from 587 nm (theoretically) to 540 nm (experimental) of the double-anion emission may be explained because of the solvation effect of the alcohol molecules, which stabilizes more the excited state than the ground state of the double anion. The formation of the ground-state double anion is also feasible, and observed experimentally as a small band to the red of the 386 nm absorption band (Figure 7, inset of Figure 10).

The generation of the polysolvate open-form molecules upon addition of alcohol to D3HF in dioxane may yield a contribution to the static quenching (Figure 8). Nevertheless, the contribution of this type of quenching is regarded as small.

The quenching mechanism of the excited state of the D3HF molecules (Scheme 4) involves the intermolecular hydrogen bond between the ethanol solvent molecules and the close-form NT of the D3HF molecule (Schemes 2 and 3). The oxygen centers of D3HF are firmed candidates to generate hydrogen

SCHEME 4

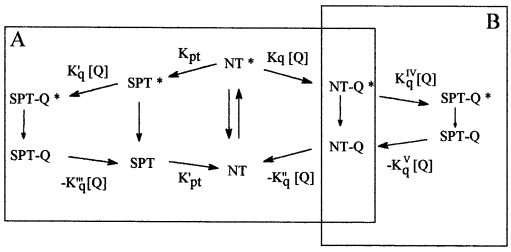

bonds, because of their increase of basicity upon excitation. In accordance to Scheme 4, upon excitation of the NT close-form tautomer two possibilities are depicted: (I) a fast PT reaction to generate the SPT tautomer and (II) the solvent molecules as quenchers might contact with the NT molecule giving rise to the formation of exciplex type species (NT-Q*). After the excited-state PT reaction, the SPT species generated undergoes several processes, for instance, (I) generation of a distinct exciplex type species that may suffer a nonradiative decay or (II) fluorescence emission. The exciplex type species SPT-Q* could comprise the complex formation of the close-form species (Scheme 2) with alcohol molecules by means of intermolecular hydrogen bonds. This represents the mechanism A in Scheme 4.

An additional mechanism B may be effective if the NT-Q* species undergoes SPT reaction before decaying, giving rise to SPT-Q* species, which may be subsequently quenched, or may emit fluorescence.

Conclusions

It is theoretically demonstrated for D3HF the interplay between the single-proton-transfer (SPT) and the double-proton-transfer (DPT) intramolecular processes in the first singlet excited state. Both proton-transfer (PT) processes are exothermic. The double-proton transfer follows a concerted mechanism. The excited-state SPT species acts as an end-point in the excited-state PT processes, and experimentally, only the SPT emission has been monitored.

As a result of density functional theory (DFT) calculations and time-dependent DFT calculations the most stable geometry for the isolated molecule corresponds to the coplanar phenyl ring conformation for both molecules D3HF and 3HF.

In dioxane solution, two fluorescence bands were recorded exhibiting identical excitation spectra that resemble the absorption spectrum of D3HF. The short-wavelength band was assigned to the normal tautomer (NT) close-form species (Scheme 2) and the long-wavelength band represents the SPT close-form species.

The addition of H-accepting solvents such as ethanol to dioxane has revealed: (a) the dynamical quenching of both the NT and the SPT fluorescences and (b) the interplay between the intramolecular SPT process and the intermolecular DPT process. This latter process is clear-cut catalyzed by the solvent molecules, thus mainly generating in the excited state the solvated double anion of the D3HF molecule.

Therefore, the long-wavelength fluorescence band at 566 nm in alcohol solution at room temperature consists of two bands: the solvated double-anion fluorescence at 540 nm, and the intramolecular SPT fluorescence at 600 nm. The overlap of this two fluorescences leads to an increase of the half-width and to a blue shift. At 77 K in glassy alcohol (e.g., ethanol), the dynamical quenching is eliminated, and the SPT fluorescence

band at 600 nm becomes dominant and separated from the solvated double-anion fluorescence.

A short-wavelength emission band is also monitored in alcohol solution. This emission band has been tentatively assigned to a close-form complex of the D3HF molecule and the alcohol molecules (i.e., Scheme 3).

Acknowledgment. We acknowledge with thanks Centro de Computación Científica of Universidad Autónoma de Madrid for computer facilities. We are greatly indebted to DGICYT of Spain (Project PB98-0063), and Florida State University for financial support. Prof. Michael Kasha and Prof. Javier Catalán are gratefully acknowledged for allowing us to use their laboratory facilities and for fruitful discussions.

Supporting Information Available: Figure 1: absorption spectra of D3HF in dioxane and Decalin, and also in ethanol. Figure 2: Stern−Volmer plot of D3HF fluorescence quenching by ethanol and dioxane. The dependence of the D3HF fluorescence ratio of the long-wavelength emission vs the temperature/viscosity ratio. Table: Intramolecular hydrogen-bond coordinates for the S_o state of the NT, SPT, and DPT tautomer molecules. This material is available free of charge via the Internet at http://pubs.acs.org.

References and Notes

(1) Harborne, J. B.; Williams, C. A. *Phytochemistry* **2000**, *55*, 481 and references therein.

(2) Chou, P. T. *J. Chin. Chem. Soc.* **2001**, *48*, 651 and references therein.

(3) Formosinho, S. J.; Arnaut, L. G. *J. Photochem. Photobiol. A: Chem.* **1993**, *75*, 21 and references therein.

(4) Barbara, P. F.; Walsh, P. K.; Brus, L. E. *J. Phys. Chem*. **1989**, *93*, 29.

(5) Falkovskaia, E.; Pivovarenko, V. G.; Del Valle, J. C. *Chem. Phys. Lett*. **2002**, *352*, 415.

(6) Sengupta, P. K.; Kasha, M. *Chem. Phys. Lett*. **1979**, *68*, 382.

(7) McMorrow, D.; Kasha, M. *J. Phys. Chem*. **1984**, *88*, 2235.

(8) Leighton, T.; Ginther, C.; Fluss, L.; Harter, W.; Causado, J.; Notario, V. In *Phenolic Compounds in Foods and Their Effects on Health II*; Huang, M. T., Ho, C. T., Lee, C. Y., Eds.; American Chemical Society Symposium Series 507; American Chemical Society: Washington, DC, 1992; p 220.

(9) Fotsis, T.; Peppov, M.; Adlercreutz, H.; Fleischmann, G.; Hare, T.; Montesano, R.; Schwigerer, L. *Proc. Natl. Acad. Sci. U.S.A.* **1993**, *90*, 2690.

(10) Coghlan, A. *New Sci.* **1998**, *14*, 14.

(11) Jankun, J.; Selman, S. H.; Swieroz, R., Jankun, E. S. *Natur*e **1997**, *287*, 561.

(12) Cao, Y.; Cao, R. *Nature* **1999**, *398*, 381.

(13) Jovanovic, S. V.; Steenven, S.; Tosic, M.; Marjanovic, B.; Simic, M. G. *J. Am. Chem. Soc.* **1999**, *116*, 4846.

(14) Rice-Evans, C. A.; Parker, L. *Flavonoids in Health and Disease*; Marcel Dekker: New York, 1998.

(15) Algar, J.; Hurley, D. E. *Proc. R. Irish Acad. B* **1936**, *43*, 83−87; *Chem. Abstr*. **1936**, *31*, 2603−2604.

(16) Hariharan, P. C.; Pople, J. A. *Chem. Phys. Lett.* **1972**, *16*, 217.

(17) **(A)** Frisch, M. J.; Trucks, G.W.; Schlegel, H. B.; Scuseria, G. E.; Robb, M. A.; Cheeseman, J. R.; Zakrzewski, V. G., Montgomery, J. A.; Stratmann, R. E.; Burant, J. C.; Dapprich, S.; Millan, J. M.; Daniels, A. D.; Kudin, K. N.; Strain, M. C.; Farkas, O.; Tomasi, J., Barone, V.; Cossi, M.; Cammi, R.; Mennuci, B.; Pomelli, C.; Adamo, C.; Clifford, S.; Ochterski, J.; Petersson, G. A.; Ayala, P. Y.; Cui, Q.; Morokuma, K.; Malick, D. K.; Rabuck, A. D.; Raghavachari, K.; Foresman, J. B.; Cioslowski, J., Ortiz, J. V.; Stefanov, B. B.; Liu, G.; Liashenko, A.; Piskorz, P.; Komaroni, I.; Gompers, R.; Martin, R. L.; Fox, D. J.; Keith, T.; Ai-Laham, M. A., Peng, C. Y.; Nanayakkara, A.; Gonzalez, C.; Challaconbe, M.; Gill, P. M. W.; Johnson, B. G.; Chen, W.; Wong, M. W.; Andrés, J. L.; Head-Gordon, M.; Replogle, E. S.; Pople, J. A. *Gaussian 98*; Gaussian, Inc.; Pittsburgh, PA, 1998. (B) *Spartan 4.1*; Wave function, Inc.: Irvine, CA, 1996.

(18) Palomar, J.; De Paz, J. L. G.; Catalán, J. *J. Phys. Chem. A* **2000**, *104*, 6453.

(19) Catalán, J.; Del Valle, J. C.; Palomar, J.; Díaz, C.; De Paz, J. L. G. *J. Phys. Chem. A* **1999**, *103*, 10921.

(20) Fulton, R. L.; Perhacs, P. *J. Phys. Chem. A* **1998**, *102*, 9001.

(21) Catalán, J. *J. Am. Chem. Soc.* **2001**, *123*, 11940. Catalán, J., Pérez, P.; Del Valle, J. C.; de Paz, J. L. G.; Kasha, M. *Proc. Natl. Acad. Sci. U.S.A.* **2002**, *99*, 5793; *Proc. Natl. Acad. Sci. U.S.A.* **2002**, *99*, 5799.

(22) Birks, J. B. In *Photophysics of Aromatic Molecules*; Wiley-Interscience John Wiley and Sons Ltd.: New York, 1970.

(23) Schwartz, B. J.; Peteanu, L. A.; Harris, C. B. *J. Phys. Chem*. **1992**, *96*, 3591.

(24) (a**)** Dick, B. *J. Phys. Chem.* **1990**, *94*, 5752. (b**)** Mühlpfordt, A.; Bultmann, T.; Ernsting, N. P.; Dick, B. *Chem. Phys*. **1994**, *181*, 447.

(25) Brucker, G. A.; Kelley, D. F. *J. Phys. Chem*. **1987**, *91*, 2856.

(26) Ben-Amotz, D.; Harris, C. B. *J. Chem. Phys*. **1987**, *86*, 4856.

(27) Itoh, M.; Fijiwara, Y. *J. Phys. Chem*. **1983**, *87*, 4558.

(28) Itoh, M.; Tanimoto, J.; Tokumura, K. *J. Am. Chem. Soc.* **1983**, *105*, 3339.

(29) Itoh, M.; Fijiwara, Y.; Sumitani, M.; Yoshihara, K. *J. Phys. Chem*. **1986**, *90*, 5672.

(30) Brewer, E. W.; Studer, S. L.; Standiford, M.; Chou, P.-T. *J. Phys. Chem*. **1989**, *93*, 6088.

(31) Sengupta, P. K.; Kasha, M. *Chem. Phys. Lett*. **1979**, *68*, 382.

(32) McMorrow, D.; Kasha, M. Proc. *Natl. Acad. Acad. Sci. U.S.A.* **1984**, *81*, 3375.

(33) Catalán, J.; Del Valle, J. C.; Díaz, C.; Palomar, J.; De Paz, J. L. G.; Kasha, M. *Int. J. Quantum Chem*. **1999**, *72*, 421.

(34) Collins, S. *J. Phys. Chem*. **1983**, *87*, 3202.

(35) Lumry, R.; Hershberg. *Photochem. Photobiol*. **1978**, *27*, 819. Song, P. S.; Kurtin, W. E. *J. Am. Chem. Soc.* **1969**, *91*, 4892. Walker, M. S.; Bednar, T. W.; Lumry, R. *J. Chem. Phys*. **1967**, *47*, 1020.

(36) Shalski, D. M.; Rayner, D. M.; Szabo, A. G. *Chem. Phys. Lett*. **1980**, *70*, 587.

(37) Eftink, M. R.; Ghiron, C. A. *J. Phys. Chem*. **1976**, *80*, 486.

(38) Mitzukuri, S.; Tonomura, T. *Proc. Imp. Acad. Tokio* **1927**, *3*, 155; *Proc. Imp. Acad. Tokio* **1932**, *5*, 155.

(39) Titani, T. *Bull. Chem. Soc. Jpn.* **1927**, *2*, 95, 161, 196, 225.